Influence of ESPAR Antenna Radiation Patterns Shape on PPCC-Based DoA Estimation Accuracy

M. Rzymowski[1] and L. Kulas[2], *Senior Member, IEEE*
Department of Microwave and Antenna Engineering
Faculty of Electronics, Telecommunications and Informatics, Gdansk University of Technology
Gdansk, Poland
[1] mateusz.rzymowski@eti.pg.gda.pl, [2] lukasz.kulas@eti.pg.gda.pl

***Abstract*—In the article, we show the influence of three different electronically steerable parasitic array radiator (ESPAR) antenna radiation patterns on the overall direction of arrival (DoA) estimation accuracy when power-pattern cross-correlation (PPCC) algorithm, relying on received signal strength (RSS) values, is used for the estimation. The ESPAR antenna designs were obtained for three optimization goals, which resulted in different radiation patterns. To check the applicability of every ESPAR antenna to wireless sensor network (WSN) applications, we have verified their achievable DoA estimation accuracy in numerical tests. The results indicate, that it is possible to provide an ESPAR antenna design for WSN applications, which have narrow radiation pattern and also provide acceptable DoA estimation accuracy.**

Keywords—Switched-beam antenna, electronically steerable parasitic array radiator (ESPAR) antenna, direction-of-arrival (DoA), received signal strength (RSS), wireless sensor network (WSN).

I. INTRODUCTION

Direction of arrival (DoA) is an important technique frequently used in modern communication systems [1]. One of the most popular methods to obtain highly accurate DoA estimation relies on digital beamforming involving many digital signal processing (DSP) units. However, such approach not only provide high resolution results, but also increases the overall energy consumption and costs [1], [2].

Electronically steerable parasitic array radiator (ESPAR) antennas provide more energy efficient alternative for DoA estimation as they are single-input structures, hence do not require multi-chain DSP units [3]. The first ESPAR antenna based DoA estimation algorithms were using a single active element surrounded by a number of parasitic elements that are connected to corresponding varactor diodes as electronically tunable reactances [4]. By applying correct bias voltages to the diodes, it is possible to shape a directional radiation pattern and rotate it around the active element and in consequence also estimate DoA of a signal impinging the antenna by recording received signal strength (RSS) values of the signal for different ESPAR antenna radiation patterns [4]. Unfortunately, to change bias voltages applied to varactor diodes in the concept proposed in [4], six digital-to-analog converters (DAC) within a DSP-based controller to provide six bias voltages with 12-bit resolution has been used. As a result, the expected energy consumption of such ESPAR antenna will be too high for inexpensive and energy efficient wireless sensor network (WSN) nodes.

To implement ESPAR antenna concept that is easily applicable to WSN nodes, one has to simplify the way the directional radiation patterns are formed and steered. To this end, based on the concept, in which parasitic elements were soldered to the ground plane or left open [5], variable impedances close to open or short circuit were proposed instead of varactor diodes [6], [7]. By such simplification in beam forming and beam steering process, it is possible to change ESPAR antenna configuration by steering RF switches that are connected to the required parasitic elements' loads (close to open or short circuit). In consequence, the proposed design can be used to provide DoA estimation or localization functionality in inexpensive WSN nodes equipped with ESPAR antennas [8], [9].

The shape of ESPAR antenna radiation patterns influence the overall DoA estimation accuracy. In the design proposed in [4], radiation patterns may be tuned by changing varactor diodes' voltage values. However, if ESPAR antenna with simplified beam steering will be chosen, one has to optimize the design with care as, after being produced, its radiation patterns cannot easily be tuned [8], [9]. Moreover, the influence of ESPAR antenna radiation patterns on DoA estimation accuracy has not been investigated so far in the available literature.

In this article, we propose three different ESPAR antenna designs with simplified beam steering and we show, how their radiation patterns shapes influence the resulting DoA estimation accuracy. To this end, we compare ESPAR antennas having maximized gain with an antenna having maximum gain in the horizontal direction and with an antenna having the lowest side lobe level (SLL). Consequently, presented results can be used by other researchers to provide ESPAR antenna designs better aligned with wireless sensor networks (WSN) nodes and their planned applications.

II. ESPAR ANTENNA DESIGNS

In the ESPAR antenna concept with a simplified beam steering [8], shown in Fig. 1, a single active monopole is fed by an SMA connector and is surrounded by twelve parasitic elements. Each of the parasitic elements is connected to the ground or opened by a corresponding SPDT (single-pole,

This work was supported by SCOTT (www.scott-project.eu) project that has received funding from the Electronic Component Systems for European Leadership Joint Undertaking under grant agreement No 737422. This Joint Undertaking receives support from the European Union's Horizon 2020 research and innovation programme and Austria, Spain, Finland, Ireland, Sweden, Germany, Poland, Portugal, Netherlands, Belgium, Norway.

double-throw) switch connected to the elements' ends at the bottom layer of the structure. Because every parasitic element connected to the ground becomes a reflector, while elements opened become directors, ESPAR antenna's radiation pattern can be configured electronically by an external microcontroller via corresponding SPDT switches. As a result, the antenna configuration can be unambiguously denoted using the steering vector $V=[\,v_1,\ v_2,\ \ldots,\ v_{12}\,]$, where v_n denotes the state of each parasitic element: $v_n=0$ for n-th parasitic element connected to the ground and 1 for opened.

The considered antenna concept has been designed in FEKO electromagnetic simulation software tool to work in WSN applications within the most popular industrial, scientific and medical (ISM) radio frequency band. To this end, the antenna has been optimized at the frequency $2.484\ GHz$ using three different optimization goals with respect to its radiation patterns. In all designs, $1.7\ mm$ height FR4 laminate with top layer metallization as its ground plane has been used.

ESPAR antenna parameters that have been optimized using the Simplex (Nelder-Mead algorithm) were distances R_1, R_2 and elements' heights h_a, h_p. In the first design, the optimization goal was to maximize the value of total gain, while the maximum value of total gain for $\theta = 90°$ was set as the optimization goal in the second one. In the third design, optimization goals included the lowest side lobe level.

The resulting values of ESPAR antenna dimensions for all the considered designs are gathered in table I, while the resulting parameters for five consecutive parasitic elements opened are in table II. The first design has considerably bigger ground plane dimensions than the two others, which influences the elevation angle value for which the maximum gain is achieved. Additionally, it can easily be noticed that the third design has considerably lower SLL levels for θ_{max} and $\theta = 90°$.

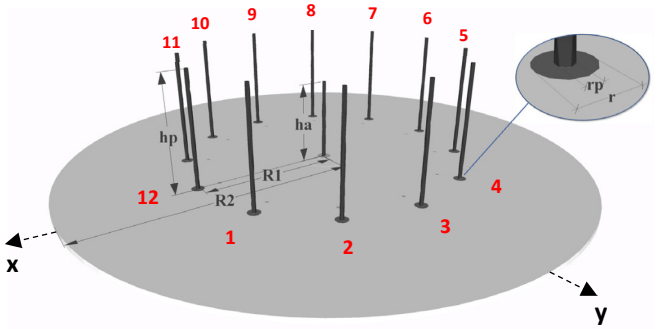

Fig. 1. Dimensions of the designed ESPAR antenna together with numbering of its parasitic elements (see text for explanations).

TABLE I
THE RESULTING VALUES OF ESPAR ANTENNA DIMENSIONS FOR THREE DIFFERENTLY OPTIMIZED DESIGNS (SEE TEXT FOR EXPLANATIONS)

	Dimension's values [mm]					
	h_a	h_p	R_1	R_2	r_p	r
Design #1	27.45 (0.22λ)	29.31 (0.24λ)	74.59 (0.60λ)	105.82 (0.85λ)	1.00 (0.01λ)	2.66 (0.21λ)
Design #2	25.79 (0.21λ)	33.07 (0.27λ)	48.74 (0.39λ)	79.97 (0.64λ)	1.00 (0.01λ)	2.66 (0.21λ)
Design #3	24.08 (0.19λ)	30.17 (0.24λ)	44.97 (0.36λ)	76.20 (0.61λ)	1.00 (0.01λ)	2.66 (0.21λ)

TABLE II
ESPAR ANTENNA'S PARAMETERS FOR THREE DIFFERENT DESIGNS SIMULATED IN FEKO AT THE CENTER FREQUENCY 2.484 GHZ

	Design #1	***Design #2***	***Design #3***
Maximum gain	10.22 dBi (θ_{max}=45°)	9.00 dBi (θ_{max}=65°)	8.31 dBi (θ_{max}=61°)
Gain at θ=90°	2.44 dBi	7.58 dBi	6.43 dBi
3dB beamwidth at θ_{max}	66°	63°	76°
3dB beamwidth at θ=90°	39°	60°	72°
SLL at θ_{max}	-9.41 dB	-10.56 dB	-16.33 dB
SLL at θ=90°	-4.08 dB	-11.53 dB	-18.43 dB

In the proposed ESPAR antenna with simplified beam steering 12 identical radiation patterns shifted by the multiple of 30° can be generated by setting five consecutive parasitic elements opened and then applying a circular shift to the steering vector V [8]. Hence, to compare the resulting radiation patterns one has to inspect them for the same steering vector in the chosen horizontal directions, which has been shown in Fig. 2.

III. DIRECTION-OF-ARRIVAL ESTIMATION USING POWER-PATTERN CROSS-CORRELATION METHOD

In order to determine, which of the considered ESPAR antenna designs enables the highest DoA estimation accuracy in WSN applications, obtained radiation patterns have to be used within a preferable DoA estimation scheme. Because simple and inexpensive RF transceivers used commonly in WSN nodes do not allow for both amplitude and phase measurements, one has to choose a method that relies on received signal strength (RSS) measurements, which can be gathered for different main beam directions. In the considered simplified beam steering case, there are 12 possible main directional beam directions $\varphi_{max}^n = \{90°, 120°, \ldots, 60°\}$ associated with the corresponding steering vectors $\{V_{max}^1, V_{max}^2, \ldots, V_{max}^{12}\}$ [8]. To obtain the main beam at $\varphi_{max}^1 = 90°$ one has to set the steering vector $V_{max}^1 = [1,1,1,1,1,0,0,0,0,0,0,0]$ as shown in Fig. 2. Then by applying circular shift to V_{max}^1 the main beam direction will be shifted by 30°. Hence, for $V_{max}^2 = [0,1,1,1,1,1,0,0,0,0,0,0]$ one obtains $\varphi_{max}^2 = 120°$, while for $V_{max}^{12} = [1,1,1,1,0,0,0,0,0,0,0,1]$ one gets $\varphi_{max}^{12} = 60°$ [8].

The power-pattern cross-correlation (PPCC) algorithm, first proposed in [4] and then adopted to be easily implementable in standard RF transceivers that are commonly used in WSN nodes [8], [9], relies only on RSS values recorded at the ESPAR antenna's output port. The PPCC algorithm relies on correlation coefficient that is calculated between ESPAR antenna radiation patterns, measured prior to the actual DoA estimation in an anechoic chamber, and RSS values recorded for the different main beam directions. In the considered case, the PPCC estimator takes the following form [8]:

$$\Gamma(\varphi) = \frac{\sum_{n=1}^{12}\left(P(V_{max}^n,\varphi)\,Y(V_{max}^n)\right)}{\sqrt{\sum_{n=1}^{12}P(V_{max}^n,\varphi)^2}\,\sqrt{\sum_{n=1}^{12}Y(V_{max}^n)^2}} \qquad (1)$$

where $\{Y(V_{max}^1), Y(V_{max}^2), \ldots, Y(V_{max}^{12})\}$ are output power values recorded during the actual estimation process for different steering vectors $\{V_{max}^1, V_{max}^2, \ldots, V_{max}^{12}\}$, while $\{P(V_{max}^1,\varphi), P(V_{max}^2,\varphi), \ldots, P(V_{max}^{12},\varphi)\}$ are ESPAR antenna's

radiation pattern values measured beforehand for all corresponding steering vectors with the angular step precision $\Delta\varphi$. Because the estimator $\Gamma(\varphi)$ is a correlation coefficient between vectors $\{P(V_{max}^1,\varphi),P(V_{max}^2,\varphi),\dots,P(V_{max}^{12},\varphi)\}$ and $\{Y(V_{max}^1),Y(V_{max}^2),\dots,Y(V_{max}^{12})\}$, the estimated DoA angle $\hat{\varphi}$ corresponds to the highest value of $\Gamma(\varphi)$ [4], [8].

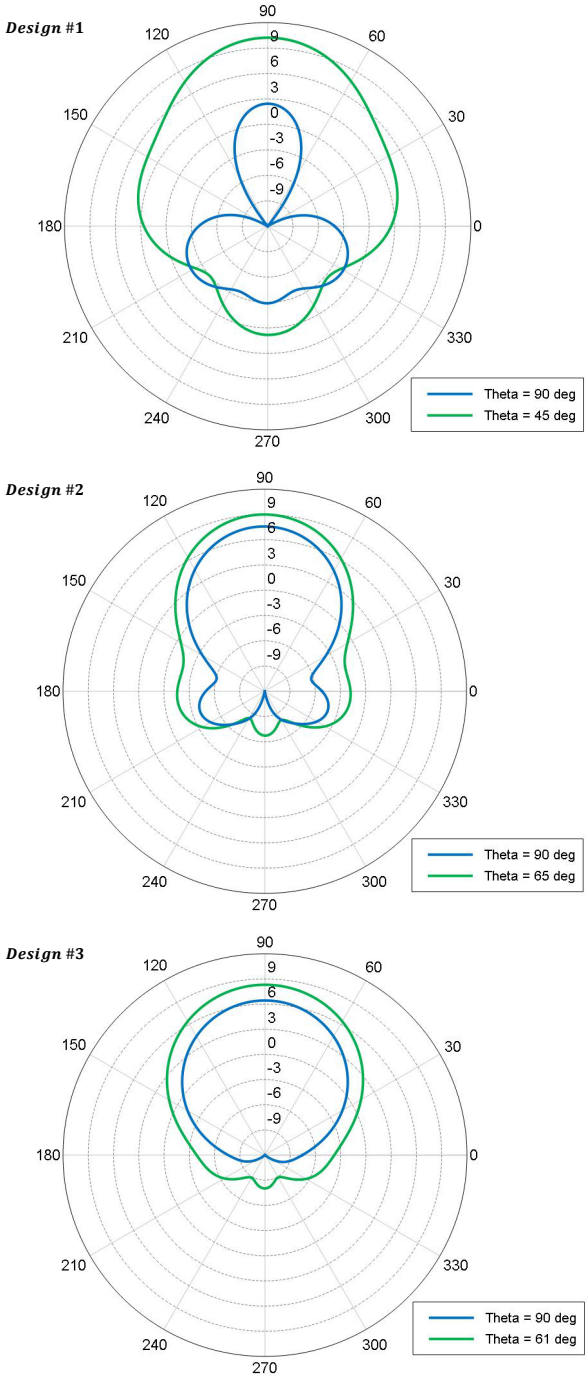

Fig. 2. ESPAR antenna's radiation patterns (in dBi) for three designs considered in the paper. In every case, main beam's direction $\varphi_{max}^1 = 90°$ is aligned with y axis and has been obtained for the steering vector $V_{max}^1 = [1,1,1,1,1,0,0,0,0,0,0,0]$ (see text for explanations).

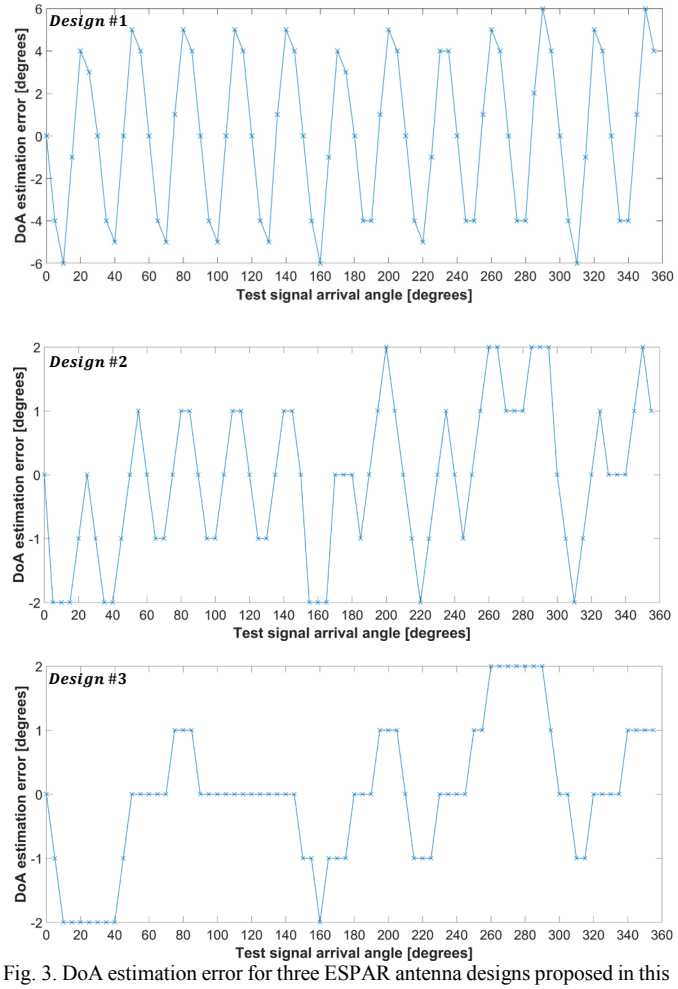

Fig. 3. DoA estimation error for three ESPAR antenna designs proposed in this paper. The results were obtained from numerical simulations using PPCC DoA estimation algorithm for SNR=10 dB (see text for explanations).

IV. Numerical Simulations

To verify, how ESPAR antenna radiation pattern shape influence the resulting DoA estimation accuracy when PPCC algorithm is used, numerical simulations were conducted. To this end, every antenna design has been simulated in a computational electromagnetic program (FEKO) to generate its radiation patterns for considered steering vectors $\{V_{max}^1,V_{max}^2,\dots,V_{max}^{12}\}$ with 1° angular step precision. As a result, 12 ESPAR antenna radiation patterns $\{P(V_{max}^1,\varphi),P(V_{max}^2,\varphi),\dots,P(V_{max}^{12},\varphi)\}$ associated with twelve main beam directions, were generated at 2.484 GHz for each of the antenna designs.

In every DoA Matlab simulation, the power of a test signal impinging the antenna has been set to $10dBm$, and the possible signal's directions has been considered with a discreet angular step equal to 5°, which is a good compromise between coarse 10° step used in [4] and very fine 1° step implemented in [9]. During the simulation, for each of 72 directions of impinging signal $\varphi_t \in \{0^\circ, 5^\circ, \dots, 355^\circ\}$, twelve output power values $\{Y(V_{max}^1),Y(V_{max}^2),\dots,Y(V_{max}^{12})\}$ were recorded for the steering vectors $\{V_{max}^1,V_{max}^2,\dots,V_{max}^{12}\}$ corresponding to directional main beam radiation patterns. Moreover, to easily compare results

with those obtained in [4] and [9], for every considered direction 10 snapshots were generated and additive white Gaussian noise has been added to all recorded output power values to generate a specific signal-to-noise ratio (SNR).

Results presented in Fig. 3 and in table III show, that ESPAR antenna radiation pattern shape has an influence the resulting PPCC algorithm DoA estimation accuracy. In the first design, error levels reach the highest value and the precision do not drop below 5° even for very low SNR. In the second and third designs, the errors have considerably lower values, but only when the third design is used, it is possible to obtain very low errors for very low SNRs. It means that, in order to provide highly accurate results, one has to design ESPAR antenna radiation patterns having very low SLL and monotonically drop from the maximum value. However, in some WSN applications DoA estimation errors obtained for the design #2 are acceptable. In such situations, one can provide ESPAR antennas for WSN nodes that have more narrow radiation patterns and 1 dB better gain by using the second design (see table II for comparison).

V. Conclusions

In the article, it has been shown, how radiation patterns of ESPAR antennas with simplified beam steering designed for WSN nodes influence the overall DoA estimation accuracy of an impinging signal. We have proposed three different ESPAR antenna designs, which were obtained for three different optimization goals. Performed numerical tests indicate, that the design with the highest gain do not provide the best DoA estimation results as in order to provide highly accurate DoA results, one has to provide a design having very low side lobe level. Moreover, as we have shown, it is possible to provide ESPAR antenna designs for WSN applications that have DoA estimation accuracy at the acceptable level and simultaneously provide radiation patterns having lower 3 dB beamwidths and higher gains.

Acknowledgment

The authors would like to thank the Academic Computer Centre in Gdansk, Poland (TASK) were all the calculations were carried out, and to the anonymous reviewers of [9] as our interesting discussions during the review process ignited the idea of using different optimization goals for ESPAR antennas used in DoA estimation, which is presented in this paper.

References

[1] Sathish Chandran, *Advances in direction-of-arrival estimation*, Artech House, London, 2005.

[2] D. H. Johnson and D. E. Dudgeon, *Array Signal Processing, Concepts and Techniques*, Englewood Cliffs, NJ: Prentice-Hall, 1993.

[3] Luis Brás, Nuno Borges Carvalho, Pedro Pinho, Lukasz Kulas, and Krzysztof Nyka, "A Review of Antennas for Indoor Positioning Systems," *International Journal of Antennas and Propagation*, vol. 2012, Article ID 953269, 14 pages, 2012.

[4] E. Taillefer, A. Hirata and T. Ohira, "Direction-of-arrival estimation using radiation power pattern with an ESPAR antenna," *IEEE Transactions on Antennas and Propagation*, vol. 53, no. 2, pp.678–684, Feb. 2005.

[5] R. Schlub and D. V. Thiel, "Switched parasitic antenna on a finite ground plane with conductive sleeve," in *IEEE Transactions on Antennas and Propagation*, vol. 52, no. 5, pp. 1343-1347, May 2004.

[6] M. Sulkowska, K. Nyka, L. Kulas, "Localization in Wireless Sensor Networks Using Switched Parasitic Antennas," *18th International Conference on Microwave Radar and Wireless Communications (MIKON 2010)*, pp.1-4, Jun. 2010.

[7] M. Rzymowski, P. Woznica and L. Kulas, "Single-Anchor Indoor Localization Using ESPAR Antenna," *IEEE Antennas Wireless Propag. Lett.*, vol. 15, pp.1183-1186, 2016.

[8] L. Kulas, "Direction-of-arrival estimation using an ESPAR antenna with simplified beam-steering," in *Proc. 47th Euro. Microw. Conf.*, Nuremberg, Germany, 2017, pp. 296–299.

[9] L. Kulas, "RSS-based DoA Estimation Using ESPAR Antennas and Interpolated Radiation Patterns," *IEEE Antennas Wireless Propag. Lett.*, vol. 17, pp.25-28, 2018.

TABLE III
DoA Estimation Errors Calculated for the Proposed ESPAR Antenna with Simplified Beam Steering Used Together with PPCC Algorithm (See Text for Explanations)

	Parameters of absolute error values				
	SNR $[dB]$	$mean$	rms	std	$precision$
Design #1	5	3.11°	3.66°	1.93°	6°
	10	3.10°	3.68°	2.00°	6°
	15	3.08°	3.73°	2.11°	6°
	20	3.03°	3.70°	2.14°	5°
	25	3.01°	3.70°	2.16°	5°
	30	3.00°	3.70°	2.18°	5°
Design #2	5	1.06°	1.41°	0.95°	3
	10	0.92°	1.18°	0.75°	2
	15	0.79°	1.01°	0.63	2
	20	0.68°	0.86°	0.53	2
	25	0.68°	0.83°	0.47	1
	30	0.67°	0.82°	0.47	1
Design #3	5	1.06	1.45	1.01	3
	10	0.76	1.09	0.78	2
	15	0.40	0.63	0.49	1
	20	0.22	0.47	0.42	1
	25	0.11	0.33	0.32	1
	30	0	0	0	0